46th Annual Review of Progress
in Quantitative Nondestructive Evaluation
QNDE2019
July 14-19, 2019, Portland, OR, USA

QNDE2019-1234

PROBABILITY OF DETECTION OF X-RAY COMPUTED TOMOGRAPHY OF ADDITIVE MANUFACTURING DEFECTS

Felix H. Kim[1], Adam L. Pintar, Jason Fox, Jared Tarr, Alkan M. Donmez
National Institute of Standards and Technology
Gaithersburg, MD, USA

Anne- Françoise Obaton
Laboratoire national de métrologie et d'essais
Paris, France

ABSTRACT

A methodology to determine probability of detection (POD) of X-ray Computed Tomography (XCT) was developed using Additive Manufacturing defects. A signal response POD analysis ($\hat{a}$ vs a) was used, where both signal response ($\hat{a}$) and true defect size (a) were the volumes of the defects. The true defect size was measured with an optical measurement system, and the measurement uncertainty of the true defect size (a) was additionally incorporated into the POD analysis. An advanced XCT image analysis method was applied to determine volume of the defect to be used as signal response ($\hat{a}$). A statistical bootstrap algorithm was used to quantify uncertainty.

Keywords: probability of detection, x-ray computed tomography, uncertainty

1. INTRODUCTION

Probability of detection (POD) is a statistical method applied to non-destructive evaluation (NDE) systems and measurements to provide reliability in the NDE systems and measurements [1]. Probability of detection analysis has been carried out on various NDE techniques including ultrasound, eddy current, and X-ray radiography, but not for XCT. This may be attributed to limited industrial application of XCT for inspection to date. A study [2] shows that XCT is the most promising method to inspect complex parts producible with metal Additive Manufacturing (AM). The high-value complex AM-produced parts are expected to be inspected for defects using XCT, and the reliability of NDE inspection with XCT must be determined.

Probability of detection is a critical component of the NDE qualification process, and it provides a clear quantitative measure of how likely an NDE system will find defects of varying size. The basic methodology for XCT POD has not been fully established yet. The definition of signal response and the choice of the decision threshold should be carefully considered. A recent study by the first two authors investigated a method to determine POD of XCT on AM defects with trapped powders [3]. Thresholded volume of the defects at a coarse and fine resolution were used for both the signal response and true defect size, respectively. The importance of setting a proper decision threshold and its relationship to critical defect size was also discussed. The defects were fully internal. In this paper, we describe new artifacts with defects that can be measured by another SI-traceable measurement technique with a rigorous uncertainty budget. The details of the measurement processes and the POD analysis process will be provided.

2. MATERIALS AND METHODS

2.1 Artifact development

Artifacts are developed in 17-4 stainless steel using laser powder bed fusion (LPBF) AM process. A rectangular defect was designed on the surface of a cylindrical artifact (10 mm dia.). Electro discharge machining (EDM) process was performed to remove rough top surfaces. A mating piece with smooth surfaces was also developed, which will make the produced defect internal when combined, and when separated the defect can be measured with a measurement system that requires the externality of features of interest. A polymer sample holder was developed using a polymer AM process to structurally hold the two pieces together while minimizing the X-ray attenuation. Constant nominal length (1 mm) and depth (40 µm) were used while varying the width of the defect from 10 µm to 1 mm to generate different volumes. The 40 µm-depth of the defect represents a layer height of the LPBF AM process. Measurable features were not developed below the 40 µm-wide defect through the AM process. Due to errors associated with aligning surfaces at the proper height with the EDM process and production limits with AM processes, the actual size of the defects deviated from the nominal design values. Total of 14 defects in rectangular shape were developed. The design and a

[1] Contact author: felix.kim@nist.gov

photograph in an assembled state of an example artifact are shown in Figures 1a and b, respectively.

2.2 Reference measurements and uncertainty quantification

An optical measurement system (Alicona InfiniteFocus G5[2]) was used with a 10x objective lens as the reference measurement technique for the defects. It provides topographical measurements (height) of the part at 0.88 µm/pixel. The volume of the defect was determined by the Alicona software's Volume Measurement module, wherein the volume of the void underneath a manually selected surface is calculated. Measurement uncertainty was estimated based on the uncertainties associated with the average height measurements and unmeasurable points in the area measurements. The measurement uncertainty ranged from 3 to 13 % of the volume measurements.

2.3 XCT measurements

XCT measurements were performed using an XCT system (North Star Imaging CXMM 50) with the parameters shown in Table. 1. The vendor supplied Feldkamp-Davis-Kress (FDK) cone beam reconstruction algorithm [4] was used to reconstruct the data. The analysis was performed using VGStudioMax v3.2 [5], and the VGEasyPore algorithm was used to threshold the defects. It is a local contrast-based local thresholding algorithm, and a procedure described in a paper of the first author [6] was used to determine the local contrast threshold input parameter. No additional filtering was performed to smooth the image. An example radiograph of the measurement is shown in Figure 1c. The small defect is not easily visible in radiograph but is clearly detectable in the XCT images as shown in the following section.

(a) (b) (c)

FIGURE 1: (a) Design of two-piece POD artifact, (b) assembled artifact in a polymer sample holder, and (c) X-ray radiograph of the POD artifact

TABLE 1: XCT acquisition parameters

Parameters	Value
Voltage (kV)	220
Current (µA)	100
Filter (material/thickness)	Cu/3 mm
Frame rate (frame/s)	3
Frames/projection	9
Number of projections	1000
Source-to-detector distance (mm)	432.3
Source-to-object distance (mm)	63.5
Geometric magnification	6.8
Detector pixel pitch (µm)	127
Effective image pixel size (µm)	18.7
Total acquisition time per sample (min)	60

3. RESULTS AND DISCUSSION

Example optical and XCT measurement results are shown in Figure 2a and b, respectively for the 100 µm-wide (nominal) defect. Both measurements clearly show the defect structures. The XCT thresholding algorithm was successfully applied to segment the defect of interest.

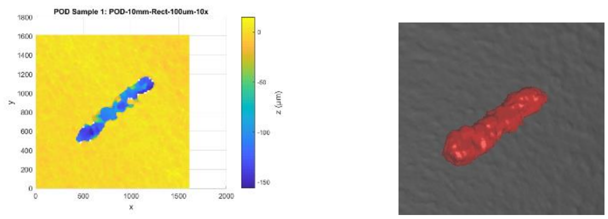

(a) (b)

FIGURE 2: (a) Optical measurement result and (b) XCT measurement result of a defect (100 µm nominal width)

A signal response POD analysis was performed based on the measurements. The $\hat{a}$ *vs* a plot is shown in Figure 3. As the measurements of $\hat{a}$ and a are both volumes of the defects, we expect a linear relationship between the two measures. A linear regression line is plotted for the 14 measurement pairs. The line was estimated on the logarithmic scale. The red line is a traditional least squares fit that does not consider uncertainty in the reference measurements (a). The black line is fitted considering uncertainty in the reference measurements (a). Both lines look quite similar for the scale of Figure 3. The pink shaded area considers uncertainty in a and deviations from linearity, and the grey shaded area considers only deviations from linearity. The decision threshold was chosen as the minimum detection capability of XCT system. We chose an 8 voxel volume following the Nyquist theorem [7], which is often used as a basis in XCT image analysis.

[2] Certain commercial equipment, instruments, or materials are identified in this paper in order to specify the experimental procedure adequately. Such identification is not intended to imply recommendation or endorsement by the National Institute of Standards and Technology, nor is it intended to imply that the materials or equipment identified are necessarily the best available for the purpose.

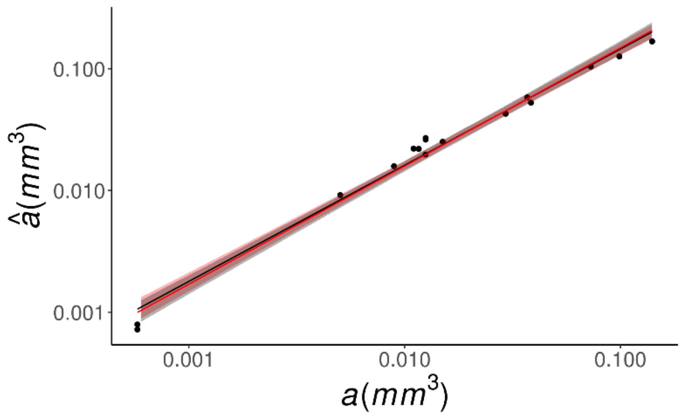

FIGURE 3: $\hat{a}$ *vs* a plot in logarithmic scale

The resulting POD curves are shown in Figure 4. The black POD curve considered the uncertainty of reference measurements. The shaded areas are the uncertainties estimated by a statistical bootstrap algorithm. The results show for this choice of threshold that the original PODs were underestimated when omitting measurement uncertainties of true defect volumes. The detailed process of implementation will be presented.

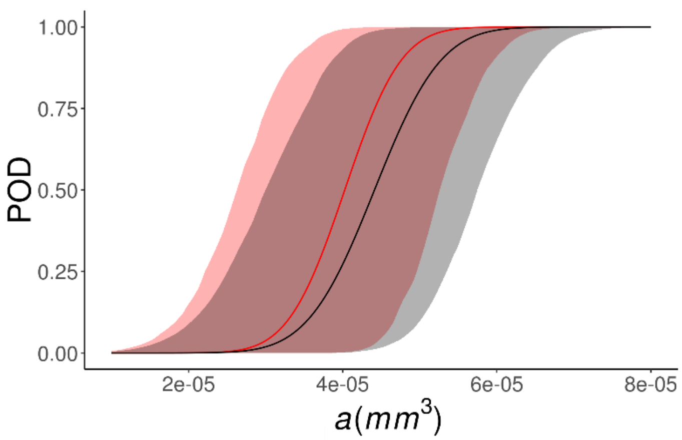

FIGURE 4: POD curves

In this paper, we chose the thresholded defect volume as the signal response. The underlying assumption is that a proper thresholding process is applied to achieve an acceptable thresholding result. The same measurement and analysis processes must be applied during the actual inspection process. The advantage of using thresholded volume is the possibility of automating the acceptance/rejection process. Different definitions of signal response based on grayscale image contrast will be explored in the future work.

4. CONCLUSION

A methodology to determine POD of XCT measurements were introduced using representative AM defects. A signal response analysis method was applied. An approach of including the measurement uncertainty of true defect was incorporated in the POD analysis. The methodology provides more accurate estimate of POD curve in the sense that all quantified sources of uncertainty are included in the analysis. In this example, the more rigorous approach improved the economy associated with the inspection process. The methodology provides a basis for future investigation of POD for more complex AM-produced components and extensions to model-assisted POD studies.

ACKNOWLEDGEMENTS

We would like to thank Dr. Jarred Heigel of NIST on discussion for developing an artifact. We would like to thank Dr. Daniel Kanzler and Dr. Sylvia Kessler for fruitful discussion on POD.

REFERENCES

[1] Berens, A., and Hovey, P., 1983, "Statistical Methods for Estimating Crack Detection Probabilities," Statistical Methods for Estimating Crack Detection Probabilities.

[2] Todorov, E., Spencer, R., Gleeson, S., Jamshidinia, M., and Kelly, S. M., 2014, "AMERICA MAKES: NATIONAL ADDITIVE MANUFACTURING INNOVATION INSTITUTE (NAMII) Project 1: Nondestructive Evaluation (NDE) of Complex Metallic Additive Manufactured (AM) Structures."

[3] Kim, F. H., Pintar, A. L., Moylan, S. P., and Garboczi, E. J., 2019, "The influence of X-ray computed tomography acquisition parameters on image quality and probability of detection of additive manufacturing defects, under review," Journal of Manufacturing Science and Engineering.

[4] Feldkamp, L. A., Davis, L. C., and Kress, J. W., 1984, "Practical cone-beam algorithm," J. Opt. Soc. Am. A, 1(6), pp. 612-619.

[5] Volume Graphics, 2018, "VG Studio Max 3.2," https://www.volumegraphics.com/.

[6] Kim, F. H., Moylan, S. P., Garboczi, E. J., and Slotwinski, J. A., 2017, "Investigation of pore structure in cobalt chrome additively manufactured parts using X-ray computed tomography and three-dimensional image analysis," Additive Manufacturing, 17, pp. 23-38.

[7] Nyquist, H., 1928, "Certain Topics in Telegraph Transmission Theory," Transactions of the American Institute of Electrical Engineers, 47(2), pp. 617-644.

